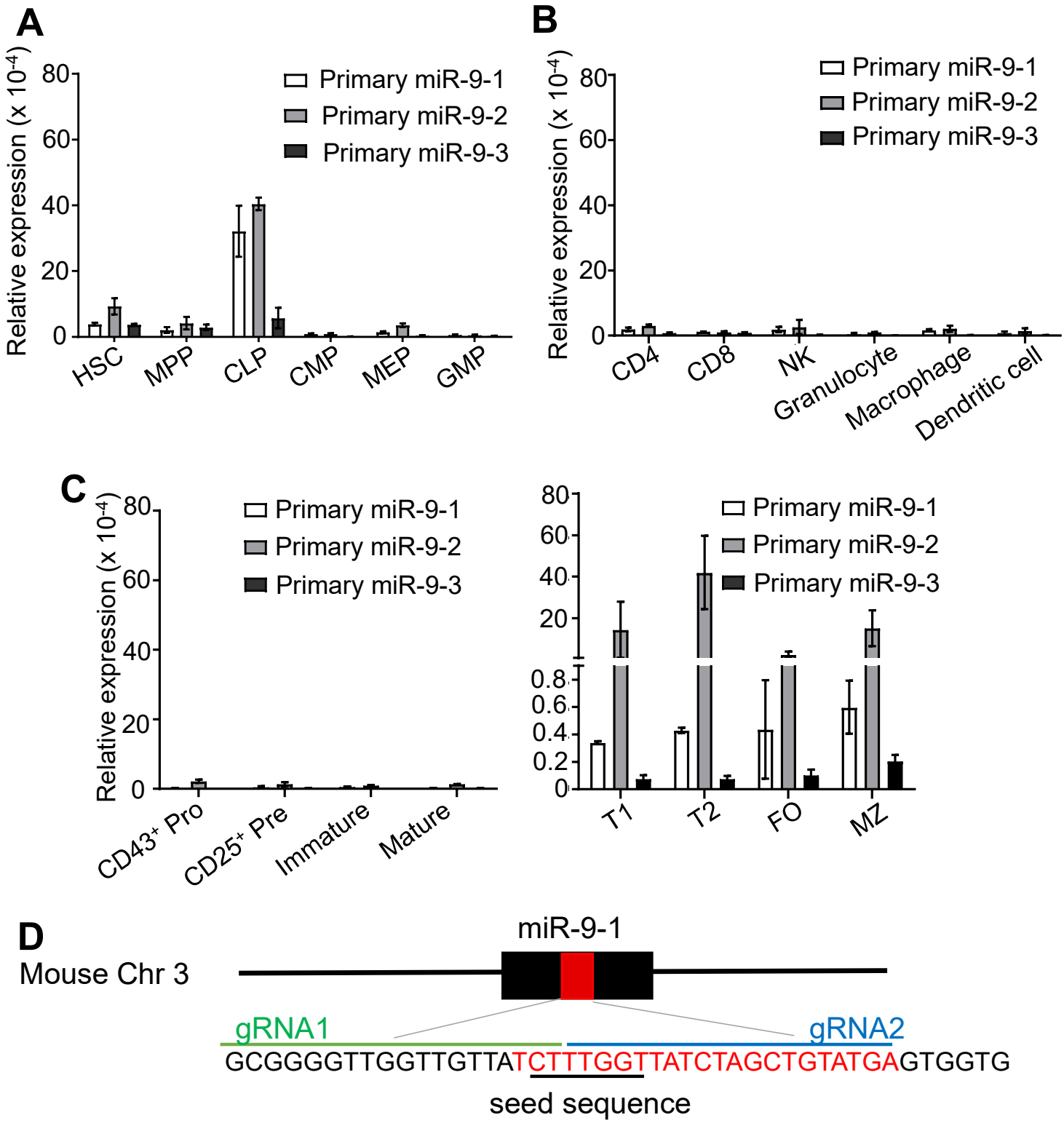
A
Relative expression (x 10-4)
80
60
40
20
0
Primary miR-9-1
Primary miR-9-2
Primary miR-9-3
HSC
MPP
CLP
CMP
MEP
GMP
B
Relative expression (x 10-4)
80
60
40
20
0
Primary miR-9-1
Primary miR-9-2
Primary miR-9-3
CD4
CD8
NK
Granulocyte
Macrophage
Dendritic cell
C
Relative expression (x 10-4)
80
60
40
20
0
Primary miR-9-1
Primary miR-9-2
Primary miR-9-3
CD43+ Pro
CD25+ Pre
Immature
Mature
80
60
40
20
0.8
0.6
0.4
0.2
0
Primary miR-9-1
Primary miR-9-2
Primary miR-9-3
T1
T2
FO
MZ
D
Mouse Chr 3
miR-9-1
gRNA1
gRNA2
GCGGGGTTGGTTGTTATCTTTGGTTATCTAGCTGTATGAGTGGTG
seed sequence
E
miR-9-1 seq
+/+ GCGGGGTTGGTTGTTATCTTTGGTTATCTAGCTGTATGAGTGGTGTGGAGT
-/- GCGGGGTTGGTTGTTAT GTATGAGTGGTGTGGAGT
miR-9-2 seq
+/+ GGGAAGCGAGTTGTTATCTTTGGTTATCTAGCTGTATGAGTGTATTGGTCTT
-/- GGGAAGCGAGTTGTTATCTTTGGTTATCTAGCTGTATGAGTGTATTGGTCTT
miR-9-3 seq
+/+ GGGAGGCCCGTTTCTCTCTTTGGTTATCTAGCTGTATGAGTGCCACAGAGC
-/- GGGAGGCCCGTTTCTCTCTTTGGTTATCTAGCTGTATGAGTGCCACAGAGC
mature miR-9

Supplementary Figure S1. Expression of miR-9-1, miR-9-2 and miR-9-3 in the different subpopulations of hematopoietic cells and generation of miR-9-1-deficient mice.

(A to C) The indicated hematopoietic progenitor subpopulations and mature hematopoietic subpopulations were sorted from wild-type mouse BM or spleen. The levels of primary miR-9-1, miR-9-2 and miR-9-3 expression were measured by qRT-PCR, using β-Actin as internal control. Mean ± SD is shown. (A) Expression of primary miR-9-1, miR-9-2 and miR-9-3 in the different subsets of BM hematopoietic progenitors. (B) Expression of primary miR-9-1, miR-9-2 and miR-9-3 in splenic CD4, CD8 and NK cells and BM granulocytes, macrophages, dendritic cells. (C) Expression of primary miR-9-1, miR-9-2 and miR-9-3 in B cells at the different developmental stages. (D) Schematic diagram of CRISPR/Cas9-mediated knockout of miR-9-1 in mice. The mouse miR-9-1 gene is located on chromosome 3. The mature miR-9 sequence is shown in red and its seed sequence is underlined. The two target sequences of gRNAs are indicated by green and blue lines above the sequences. (E) DNA sequencing analysis of miR-9-1, miR-9-2 and miR-9-3 genes in miR-9-1-deficient (-/-) and wild-type (+/+) mice. The mature miR-9 sequence is shown in red. Data shown are representative of 3 independent experiments (A to C).

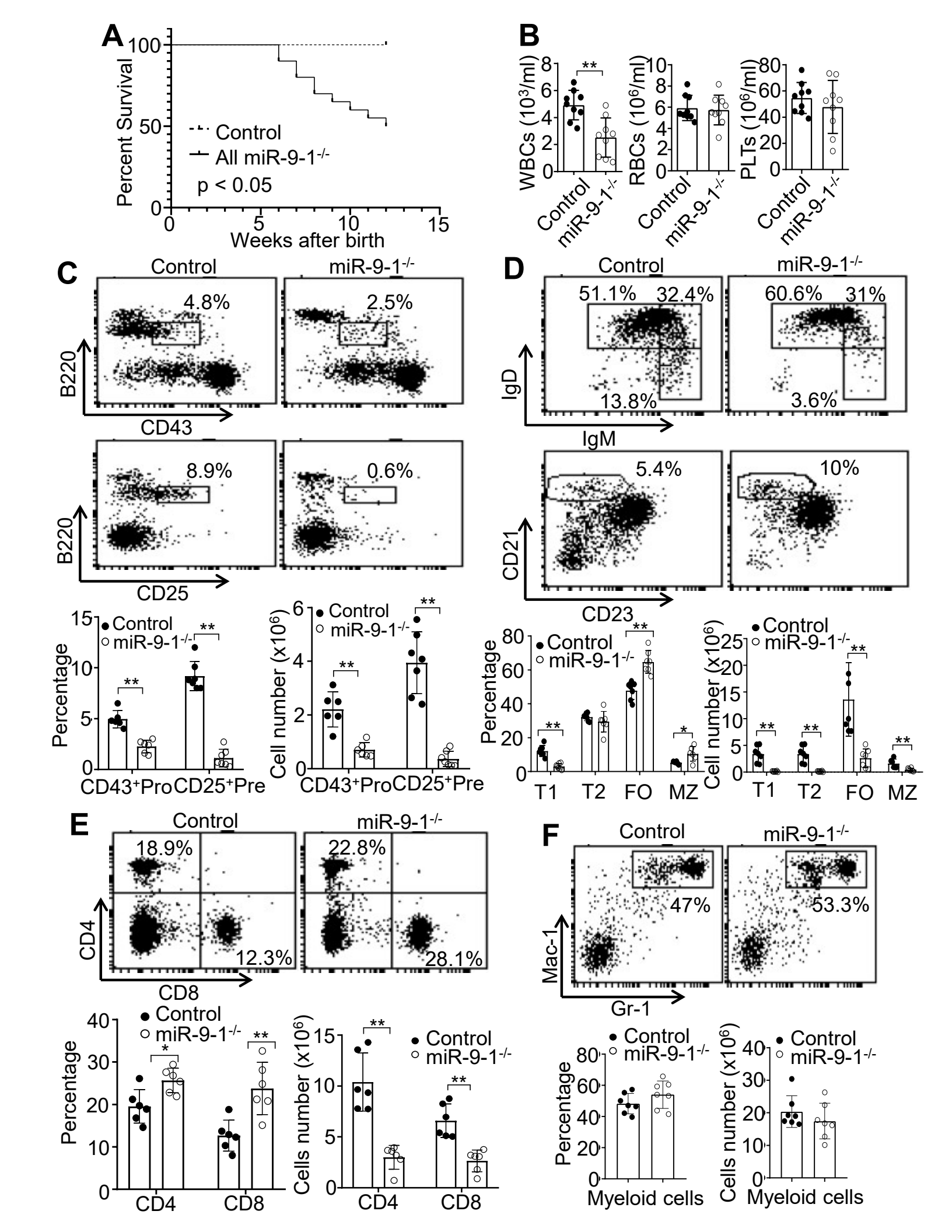
A
Percent Survival
Control
All miR-9-1-/-
p < 0.05
Weeks after birth
B
WBCs (10³/ml)
RBCs (10⁶/ml)
PLTs (10⁶/ml)
Control
miR-9-1-/-
C
Control
miR-9-1-/-
4.8%
2.5%
B220
CD43
8.9%
0.6%
CD25
Percentage
Cell number (x10⁶)
CD43⁺ProCD25⁺Pre
D
51.1%
32.4%
60.6%
31%
13.8%
3.6%
IgD
IgM
5.4%
10%
CD21
CD23
T1
T2
FO
MZ
E
18.9%
22.8%
12.3%
28.1%
CD4
CD8
Cells number (x10⁶)
F
47%
53.3%
Mac-1
Gr-1
Myeloid cells

Supplementary Figure S2. Reduced survival, white blood cells, and T and B cell populations but normal myeloid cell population in miR-9-1-deficient mice.

(A) Cumulative survival curve of all miR-9-1-deficient mice. (B) Numbers of white blood cells (WBCs), red blood cells (RBCs) and platelets (PLTs) in the peripheral blood of miR-9-1-deficient mice with retarded growth. (C) Reduction in pro- and pre-B cells in the BM of miR-9-1-deficient mice. BM cells from growth-retarded miR-9-1$^{-/-}$ and control mice were stained with anti-B220, anti-IgM, and anti-CD43 or anti-CD25. Percentages and numbers of pro- and pre-B cells in the BM are shown, and percentages indicate cells in the gated live cells. (D) Reduction in T1, T2, FO and MZ B cells in the spleen of miR-9-1-deficient mice. Splenocytes from growth-retarded miR-9-1$^{-/-}$ and control mice were stained with anti-B220, anti-IgD, anti-IgM, anti-CD21 and anti-CD23. Percentages and numbers of T1, T2, FO and MZ B cells in the spleen are shown, and percentages indicate cells in the gated B220^{+} cells. (E) Reduced T cells in the spleen of miR-9-1-deficient mice. Splenocytes from growth-retarded miR-9-1$^{-/-}$ and control mice were stained with anti-CD4 and anti-CD8. Percentages and numbers of CD4^{+} and CD8^{+} T cells in the spleen are shown and percentages indicate cells in the gated live cells. (F) Normal myeloid cell population in the BM of miR-9-1-deficient mice. BM cells from growth-retarded miR-9-1$^{-/-}$ and control mice were stained with anti-Mac-1 and anti-Gr-1. Percentages and numbers of Mac-1^{+}Gr-1^{+} myeloid cells in the BM are shown and percentages indicate cells in the gated live cells. Data shown are representative of or obtained from 20 (A), 9 (B), 7 (C, D), 6 (E) or 7 (F) pairs of control and miR-9-1$^{-/-}$ mice. Each dot represents an individual mouse. Mean $\pm$ SD is shown. *, $p < 0.05$; **, $p < 0.01$.

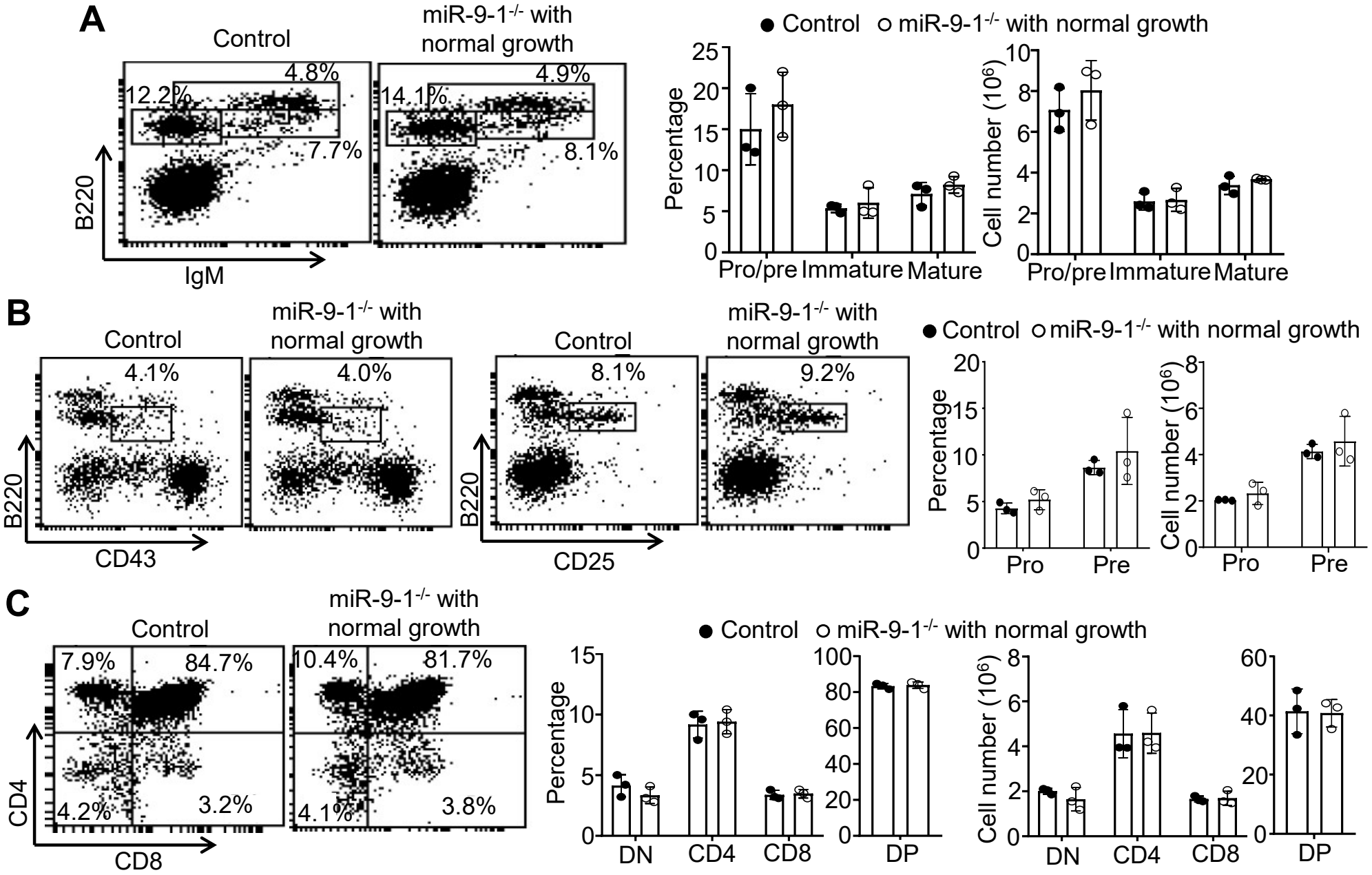
A
Control
miR-9-1-/- with normal growth
4.8%
12.2%
7.7%
4.9%
14.1%
8.1%
B220
IgM
● Control ○ miR-9-1-/- with normal growth
Percentage
Cell number (10^6)
Pro/pre
Immature
Mature
B
Control
miR-9-1-/- with normal growth
4.1%
4.0%
8.1%
9.2%
B220
CD43
CD25
● Control ○ miR-9-1-/- with normal growth
Percentage
Cell number (10^6)
Pro
Pre
C
Control
miR-9-1-/- with normal growth
7.9%
84.7%
4.2%
3.2%
10.4%
81.7%
4.1%
3.8%
CD4
CD8
● Control ○ miR-9-1-/- with normal growth
Percentage
Cell number (10^6)
DN
CD4
CD8
DP

Supplementary Figure S3. Normal lymphopoiesis in miR-9-1-deficient mice with normal growth.
(A) Normal pro/pre-, immature and mature B cell populations in the BM of miR-9-1-deficient mice with normal growth. BM cells from miR-9-1$^{-/-}$ mice with normal growth and wild-type control mice were stained with anti-B220 and anti-IgM. Percentages and numbers of pro/pre-, immature and mature B cells in the BM are shown and percentages indicate cells in the gated live cells. (B) Normal pro- and pre-B cell populations in the BM of miR-9-1-deficient mice with normal growth. BM cells from miR-9-1$^{-/-}$ mice with normal growth and wild-type control mice were stained with anti-B220, anti-IgM, and anti-CD43 or anti-CD25. Percentages and numbers of pro- and pre-B cells in the BM are shown and percentages indicate cells in the gated live cells. (C) Normal DN, DP and SP T cells in the thymus of miR-9-1-deficient mice with normal growth. Thymocytes from normal miR-9-1$^{-/-}$ and control mice were stained with anti-CD4 and anti-CD8. Percentages and numbers of DN, DP and SP T cells in the thymus are shown and percentages indicate cells in the gated live cells. Data shown are representative of or obtained from 3 miR-9-1$^{-/-}$ mice with normal growth and wild-type control mice. Each dot represents an individual mouse. Mean $\pm$ SD is shown.

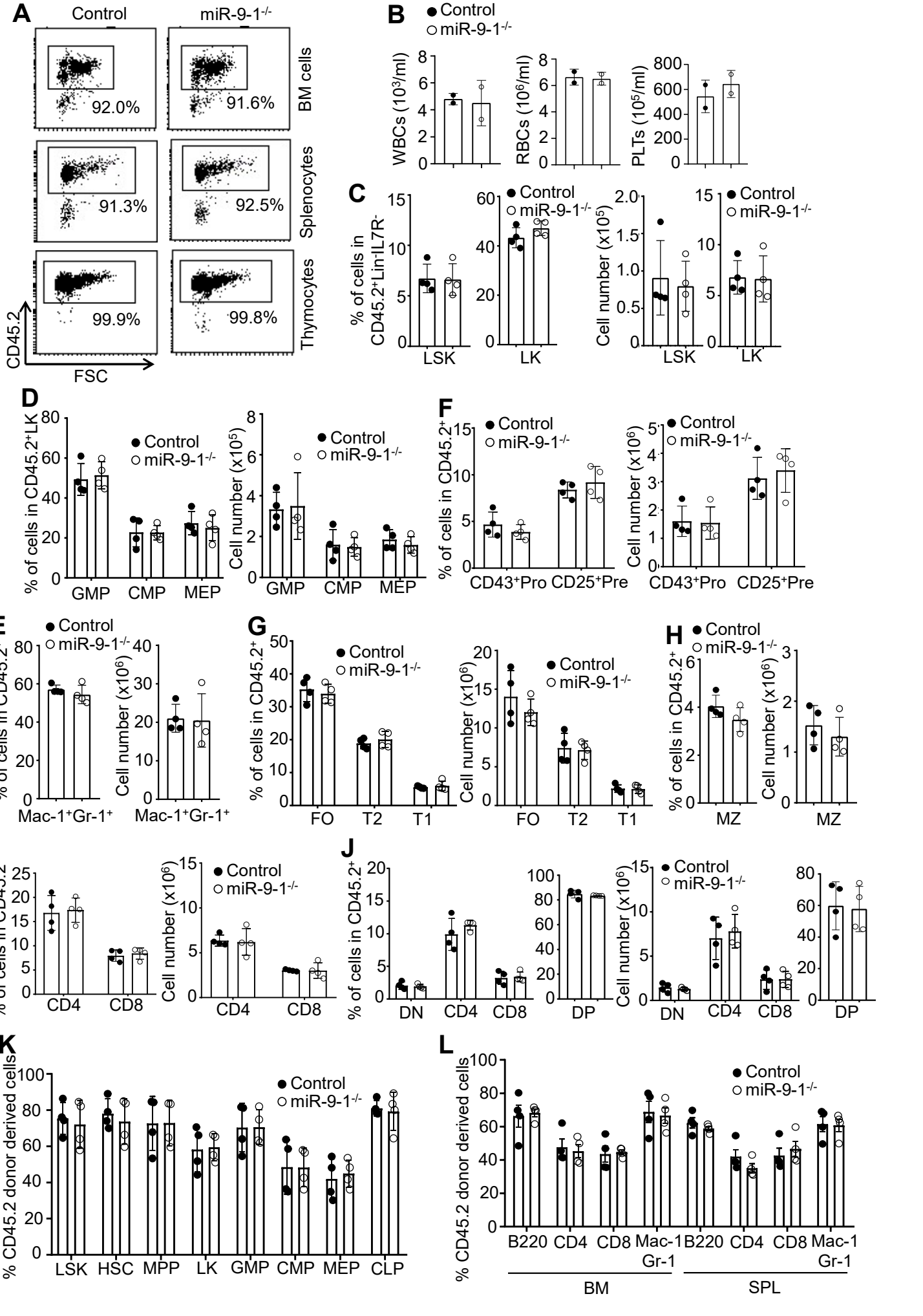
A
Control
miR-9-1-/-
92.0%
91.6%
BM cells
91.3%
92.5%
Splenocytes
99.9%
99.8%
Thymocytes
CD45.2
FSC
B
Control
miR-9-1-/-
WBCs (10³/ml)
RBCs (10⁶/ml)
PLTs (10⁵/ml)
C
% of cells in CD45.2⁺Lin⁻IL7R⁻
Cell number (x10⁵)
LSK
LK
D
% of cells in CD45.2⁺LK
Cell number (x10⁵)
GMP
CMP
MEP
E
% of cells in CD45.2⁺
Cell number (x10⁶)
Mac-1⁺Gr-1⁺
F
% of cells in CD45.2⁺
Cell number (x10⁶)
CD43⁺Pro
CD25⁺Pre
G
% of cells in CD45.2⁺
Cell number (x10⁶)
FO
T2
T1
H
% of cells in CD45.2⁺
Cell number (x10⁶)
MZ
I
% of cells in CD45.2⁺
Cell number (x10⁶)
CD4
CD8
J
% of cells in CD45.2⁺
Cell number (x10⁶)
DN
CD4
CD8
DP
K
% CD45.2 donor derived cells
LSK
HSC
MPP
LK
GMP
CMP
MEP
CLP
L
% CD45.2 donor derived cells
B220
CD4
CD8
Mac-1
Gr-1
BM
SPL

Supplementary Figure S4. Normal hematopoietic progenitors, lymphocytes and myeloid cells in the recipients that received BM cells from growth-retarded miR-9-1-deficient mice.

BM cells from wild-type control or growth-retarded miR-9-1$^{-/-}$ mice (CD45.2^{+}) were transplanted into lethally irradiated CD45.1^{+} recipients. About eight weeks after transplantation, the recipients were analyzed. (A) The percentages of CD45.2^{+} cells in the BM, spleens and thymi of the recipients. Percentages indicate CD45.2^{+} cells in the gated live cells. (B) The numbers of white blood cells (WBCs), red blood cells (RBCs) and platelets (PLTs) in the peripheral blood of the recipients. (C) The percentages and numbers of CD45.2^{+} LSK and LK cells in the BM of the recipients. Percentages indicate CD45.2^{+} LSK and LK in the gated CD45.2^{+}Lin^{-}IL-7R^{-} population. (D) The percentages and numbers of GMP, CMP and MEP in the BM of the recipients. Percentages indicate GMP, CMP and MEP in the gated CD45.2^{+}Lin^{-}IL-7R^{-} LK population. (E) The percentages and numbers of Mac-1^{+}Gr-1^{+} myeloid cells in the BM of the recipients. Percentages indicate Mac-1^{+}Gr-1^{+} myeloid cells in the gated CD45.2^{+} population. (F) The percentages and numbers of pro- and pre-B cells in the BM of the recipients. Percentages indicate CD43^{+} pro- and CD25^{+} pre-B cells in the gated CD45.2^{+} population. (G,H) The percentages and numbers of B cells at the different developmental stages in the spleen of the recipients. Percentages indicate FO, T2, T1 and MZ B cells in the gated CD45.2^{+}B220^{+} population. (I) The percentages and numbers of CD4^{+} and CD8^{+} T cells in the spleen of the recipients. Percentages indicate CD4^{+} and CD8^{+} T cells in the gated CD45.2^{+} population. (J) The percentages and numbers of DN, DP and SP T cells in the thymus of the recipients. Percentages indicate DN, DP and SP T cells in the gated CD45.2^{+} population. (K,L) Normal engrafting capacity of miR-9-1-deficient hematopoietic progenitors. BM cells from wild-type or growth-retarded miR-9-1$^{-/-}$ mice (CD45.2^{+}) were mixed 1:1 with wild-type competitor BM cells from B6 SJL mice (CD45.1^{+}) and transplanted into lethally irradiated CD45.1^{+} mice. Eight weeks after BM transplantation, the recipients were analyzed for the relative contribution of donor engraftment in various hematopoietic progenitors in the BM (K) and splenic T, B and myeloid cells (L). Data shown are obtained from 4 (A, C to J) or 2 (B) recipients that received control or miR-9-1$^{-/-}$ BM cells or 4 (K, L) recipients that received control or miR-9-1$^{-/-}$ BM cells mixed at a 1:1 ratio with competitor BM cells from wild-type B6 SJL mice (CD45.1^{+}). Each dot represents an individual mouse. Mean $\pm$ SD is shown. *, $p < 0.05$; **, $p < 0.01$.

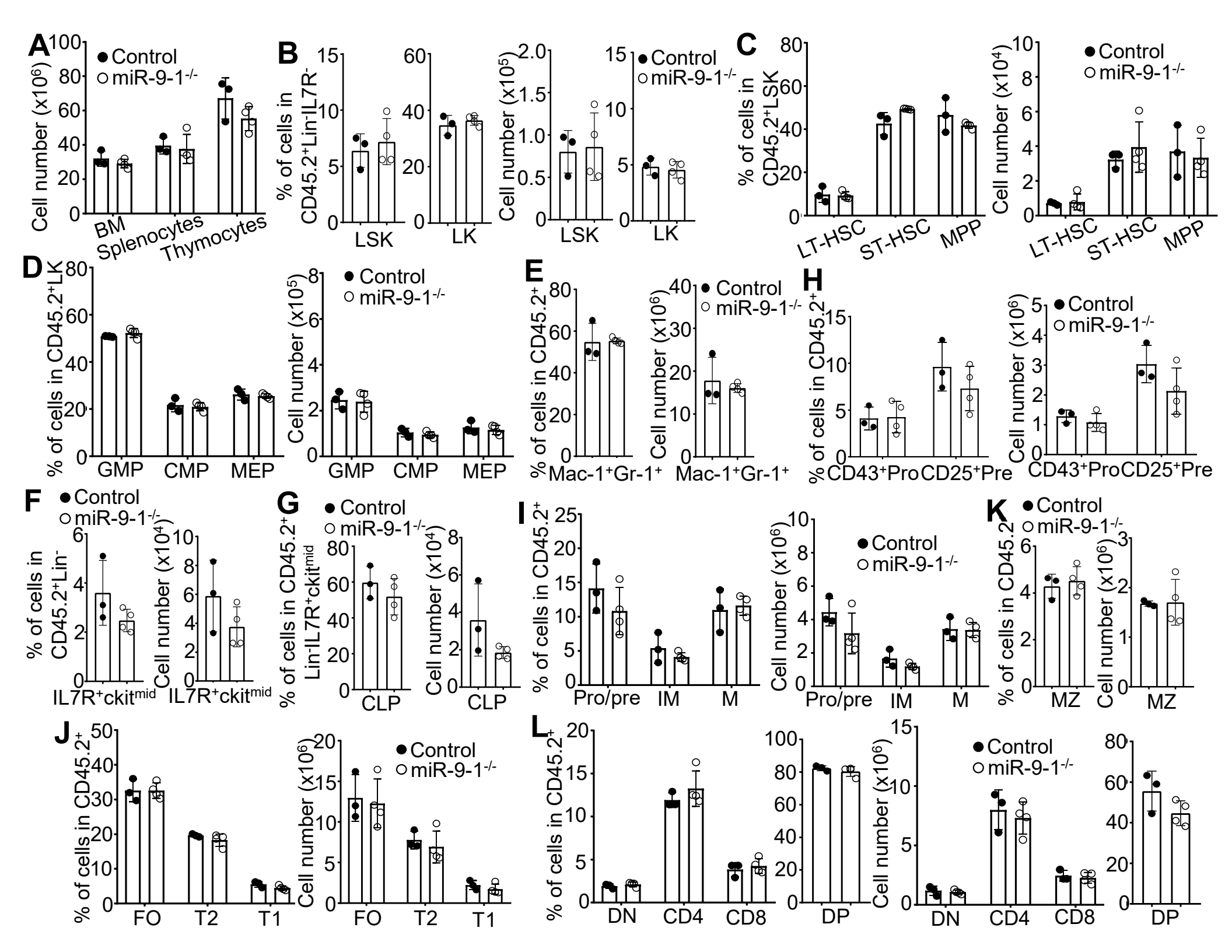
A
Cell number (x10^6)
Control
miR-9-1^-/-
BM
Splenocytes
Thymocytes
B
% of cells in CD45.2^+Lin^-IL7R^-
LSK
LK
Cell number (x10^5)
C
% of cells in CD45.2^+LSK
LT-HSC
ST-HSC
MPP
Cell number (x10^4)
D
% of cells in CD45.2^+LK
GMP
CMP
MEP
Cell number (x10^5)
E
% of cells in CD45.2^+
Mac-1^+Gr-1^+
Cell number (x10^6)
H
% of cells in CD45.2^+
CD43^+Pro
CD25^+Pre
Cell number (x10^6)
F
% of cells in CD45.2^+Lin^-
IL7R^+ckit^mid
Cell number (x10^4)
G
% of cells in CD45.2^+ Lin^-IL7R^+ckit^mid
CLP
Cell number (x10^4)
I
% of cells in CD45.2^+
Pro/pre
IM
M
Cell number (x10^6)
K
% of cells in CD45.2^+
MZ
Cell number (x10^6)
J
% of cells in CD45.2^+
FO
T2
T1
Cell number (x10^6)
L
% of cells in CD45.2^+
DN
CD4
CD8
DP
Cell number (x10^6)

Supplementary Figure S5. Normal hematopoietic progenitors, lymphocytes and myeloid cells in the recipients that received BM cells from growth-retarded miR-9-1-deficient mice after 12 weeks.

BM cells from wild-type control or growth-retarded miR-9-1$^{-/-}$ mice (CD45.2^{+}) were transplanted into lethally irradiated CD45.1^{+} recipients. Twelve weeks after transplantation, the recipients were analyzed. (A) The numbers of total BM cells, splenocytes and thymocytes the recipients. (B) The percentages and numbers of CD45.2^{+} LSK and LK cells in in the BM of the recipients. Percentages indicate CD45.2^{+} LSK and LK in the gated CD45.2^{+}Lin^{-}IL-7R^{-} population. (C) The percentages and numbers of LT-HSC, ST-HSC and MPP in the recipients. Percentages indicate LT-HSC, ST-HSC and MPP in the gated CD45.2^{+}Lin^{-}IL-7R^{-} LSK population. (D) The percentages and numbers of GMP, CMP and MEP in the BM of the recipients. Percentages indicate GMP, CMP and MEP in the gated CD45.2^{+}Lin^{-}IL-7R^{-} LK population. (E) The percentages and numbers of Mac-1^{+}Gr-1^{+} myeloid cells in the BM of the recipients. Percentages indicate Mac-1^{+}Gr-1^{+} myeloid cells in the gated CD45.2^{+} population. (F,G) The percentages and numbers of lymphoid progenitors in the BM of the recipients. Percentages indicate IL7R^{+}ckit^{mid} in the gated CD45.2^{+}Lin^{-} population (F) and CLP in the gated CD45.2^{+}Lin^{-}IL7R^{+}ckit^{mid} population (G). (H) The percentages and numbers of pro- and pre-B cells in the BM of the recipients. Percentages indicate CD43^{+} pro- and CD25^{+} pre-B cells in the gated CD45.2^{+} population. (I) The percentages and numbers of B cells at the different developmental stages in the BM of the recipients. Percentages indicate pro/pre-, immature (IM) and mature (M) B cells in the gated CD45.2^{+} population. (J,K) The percentages and numbers of B cells at the different developmental stages in the spleen of the recipients. Percentages indicate FO, T2, T1 (J) and MZ (K) B cells in the gated CD45.2^{+}B220^{+} population. (L) The percentages and numbers of DN, DP and SP T cells in the thymus of the recipients. Percentages indicate DN, DP and SP T cells in the gated CD45.2^{+} population. Data shown are obtained from 3 recipients that received control BM cells and 4 recipients that received miR-9-1$^{-/-}$ BM cells. Each dot represents an individual mouse. Mean $\pm$ SD is shown. *, $p < 0.05$; **, $p < 0.01$.

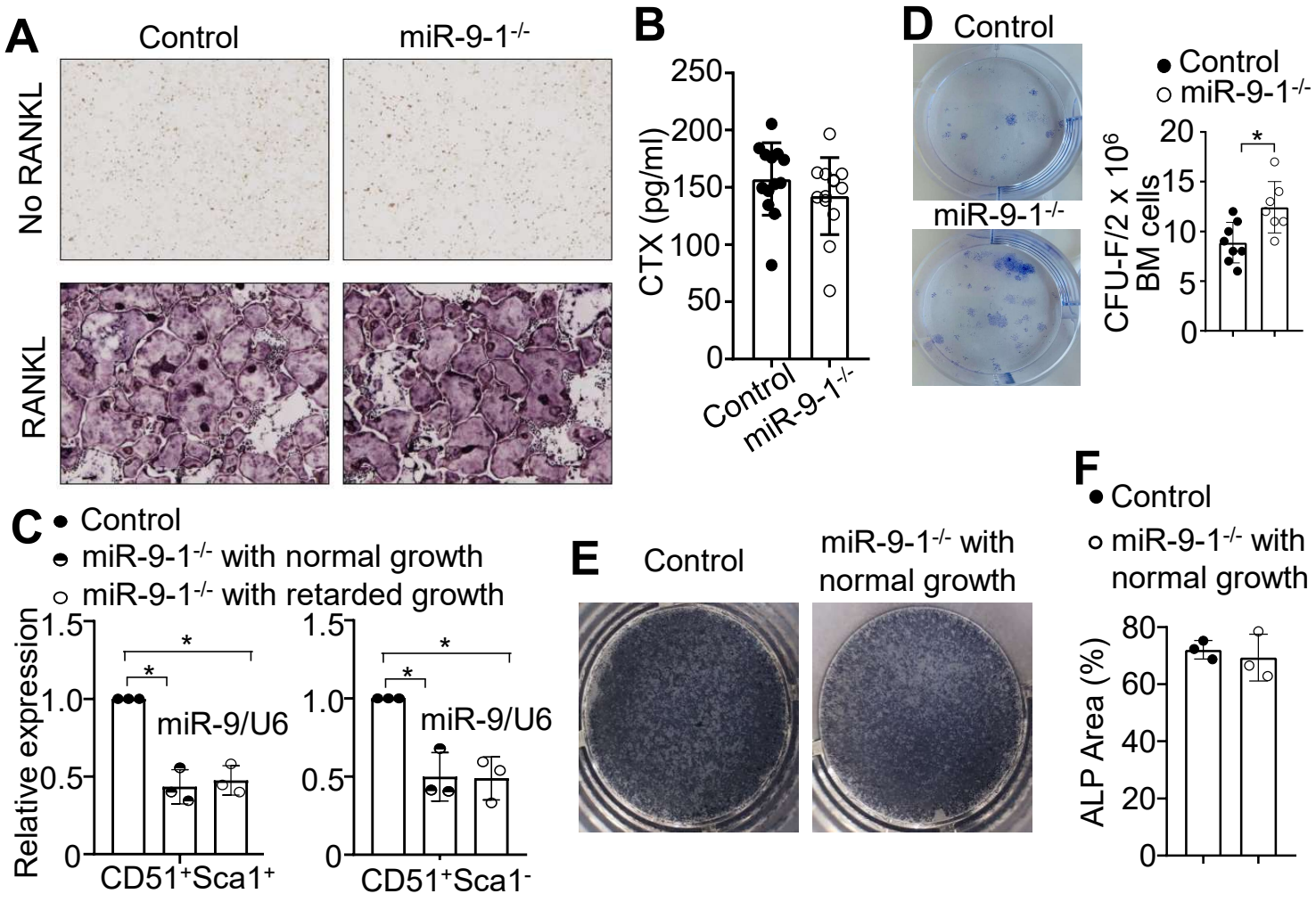

Supplementary Figure S6. Normal osteogenic differentiation of MSCs from miR-9-1-deficient mice with retarded growth or normal growth.

(A) RANKL-induced osteoclast differentiation of miR-9-1-deficient BMMs in vitro. BMMs derived from growth-retarded miR-9-1$^{-/-}$ and control mice were cultured with RANKL and M-CSF. The cells were stained with TRAP staining and visualized by light microscopy. (B) Serum level of CTX in miR-9-1-deficient mice. Serum levels of CTX in 6-12 weeks old growth-retarded miR-9-1$^{-/-}$ and control mice were determined by the ELISA analysis. (C) Marked reduction of the level of total mature miR-9 in miR-9-1-deficient CD51^{+}Sca1^{+} MSCs and CD51^{+}Sca1^{-} OBs. The relative levels of total mature miR-9 in CD51^{+}Sca1^{+} and CD51^{+}Sca1^{-} cells from the BM of miR-9-1$^{-/-}$ mice with normal or retarded growth were quantified by qRT-PCR as a fraction of the corresponding wild-type control cells, which was set as 1. (D) CFU-F formation of miR-9-1-deficient MSCs. MSCs isolated from the BM of miR-9-1$^{-/-}$ and control mice were subjected to the CFU-F assay. Morphology of CFU-Fs stained with crystal violet (left) and quantification of CFU-F numbers (right) are shown. (E, F) MSCs sorted from miR-9-1$^{-/-}$ mice with normal growth and wild-type controls were cultured in osteogenic media for 7 days, and ALP staining (A) and quantification (B) were performed. Data shown are representative of or obtained from 2 (A), 13 (B), 3 (C), 8 (D) miR-9-1$^{-/-}$ and control mice or representative of or obtained from 3 (E, F) independent experiments. Mean ± SD is shown.

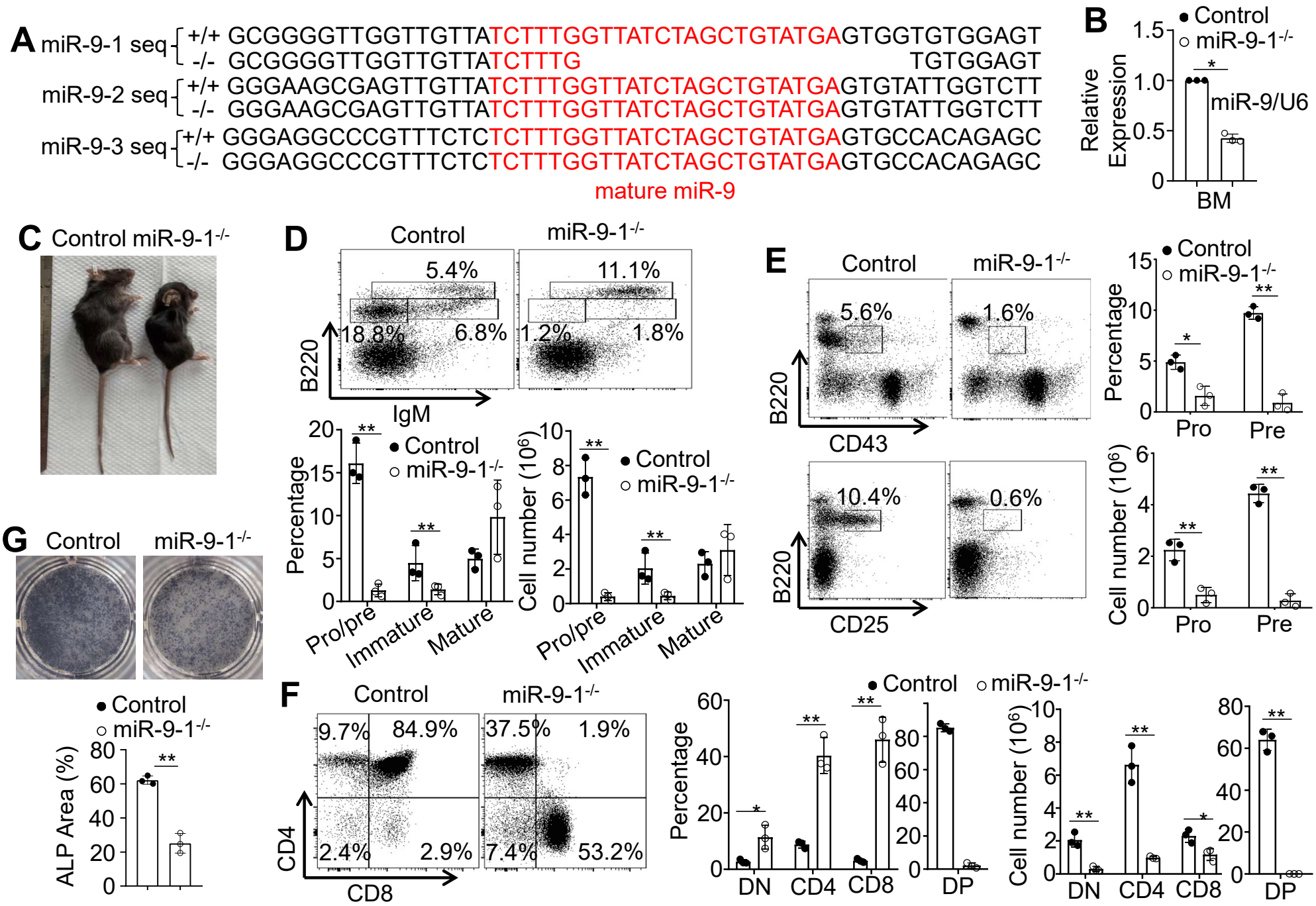
A
miR-9-1 seq
+/+ GCGGGGTTGGTTGTTATCTTTGGTTATCTAGCTGTATGAGTGGTGTGGAGT
-/- GCGGGGTTGGTTGTTATCTTTG TGTGGAGT
miR-9-2 seq
+/+ GGGAAGCGAGTTGTTATCTTTGGTTATCTAGCTGTATGAGTGTATTGGTCTT
-/- GGGAAGCGAGTTGTTATCTTTGGTTATCTAGCTGTATGAGTGTATTGGTCTT
miR-9-3 seq
+/+ GGGAGGCCCGTTTCTCTCTTTGGTTATCTAGCTGTATGAGTGCCACAGAGC
-/- GGGAGGCCCGTTTCTCTCTTTGGTTATCTAGCTGTATGAGTGCCACAGAGC
mature miR-9
B
Control
miR-9-1-/-
Relative Expression
miR-9/U6
BM
C
Control miR-9-1-/-
D
Control
miR-9-1-/-
5.4%
11.1%
18.8%
6.8%
1.2%
1.8%
B220
IgM
Percentage
Cell number (10^6)
Pro/pre
Immature
Mature
E
Control
miR-9-1-/-
5.6%
1.6%
10.4%
0.6%
B220
CD43
CD25
Percentage
Cell number (10^6)
Pro
Pre
G
Control
miR-9-1-/-
ALP Area (%)
F
Control
miR-9-1-/-
9.7%
84.9%
37.5%
1.9%
2.4%
2.9%
7.4%
53.2%
CD4
CD8
Percentage
Cell number (10^6)
DN
CD4
CD8
DP

Supplementary Figure S7. Analysis of the 2nd independent colony of miR-9-1-deficient mice.
(A) DNA sequencing analysis of miR-9-1, miR-9-2 and miR-9-3 genes in miR-9-1-deficient (-/-) and wild-type (+/+) mice of the 2nd independent colony. The mature miR-9 sequence is shown in red. (B) Reduction in overall mature miR-9 expression in the BM of growth-retarded miR-9-1-deficient mice from the 2nd independent colony. The levels of mature miR-9 expression in BM cells from miR-9-1-deficient (miR-9-1-/-) mice were quantified by qRT-PCR as a fraction of the corresponding wild-type control cells, which was set as 1. (C) Growth defect in miR-9-1-deficient mice from the 2nd independent colony. A representative image of 8-week-old growth-retarded male miR-9-1$^{-/-}$ mice and controls is shown. (D) Reduction in pro/pre- and immature B cells in the BM of growth-retarded miR-9-1-deficient mice from the 2nd independent colony. BM cells from growth-retarded miR-9-1$^{-/-}$ and control mice were stained with anti-B220 and anti-IgM. Percentages and numbers of pro/pre-, immature and mature B cells in the BM are shown, and percentages indicate cells in the gated live cells. (E) Reduction in pro- and pre-B cells in the BM of growth-retarded miR-9-1-deficient mice from the 2nd independent colony. BM cells from growth-retarded miR-9-1$^{-/-}$ and control mice were stained with anti-B220, anti-IgM, and anti-CD43 or anti-CD25. Percentages and numbers of pro- and pre-B cells in the BM are shown, and percentages indicate cells in the gated live cells. (F) Reduction in DN, DP and SP T cells in the thymus of growth-retarded miR-9-1-deficient mice from the 2nd independent colony. Thymocytes from growth-retarded miR-9-1$^{-/-}$ and control mice were stained with anti-CD4 and anti-CD8. Percentages and numbers of DN, DP and SP T cells in the thymus are shown, and percentages indicate cells in the gated live cells. (G) ALP staining of miR-9-1-deficient MSCs from the 2nd independent colony after osteogenic differentiation. MiR-9-1$^{-/-}$ and control MSCs were cultured in osteogenic media for 7 days, and ALP staining (top) and quantification (bottom) were performed. Data shown are representative of or obtained from 3 independent experiments. Mean $\pm$ SD is shown. *, $p < 0.05$; **, $p < 0.01$.

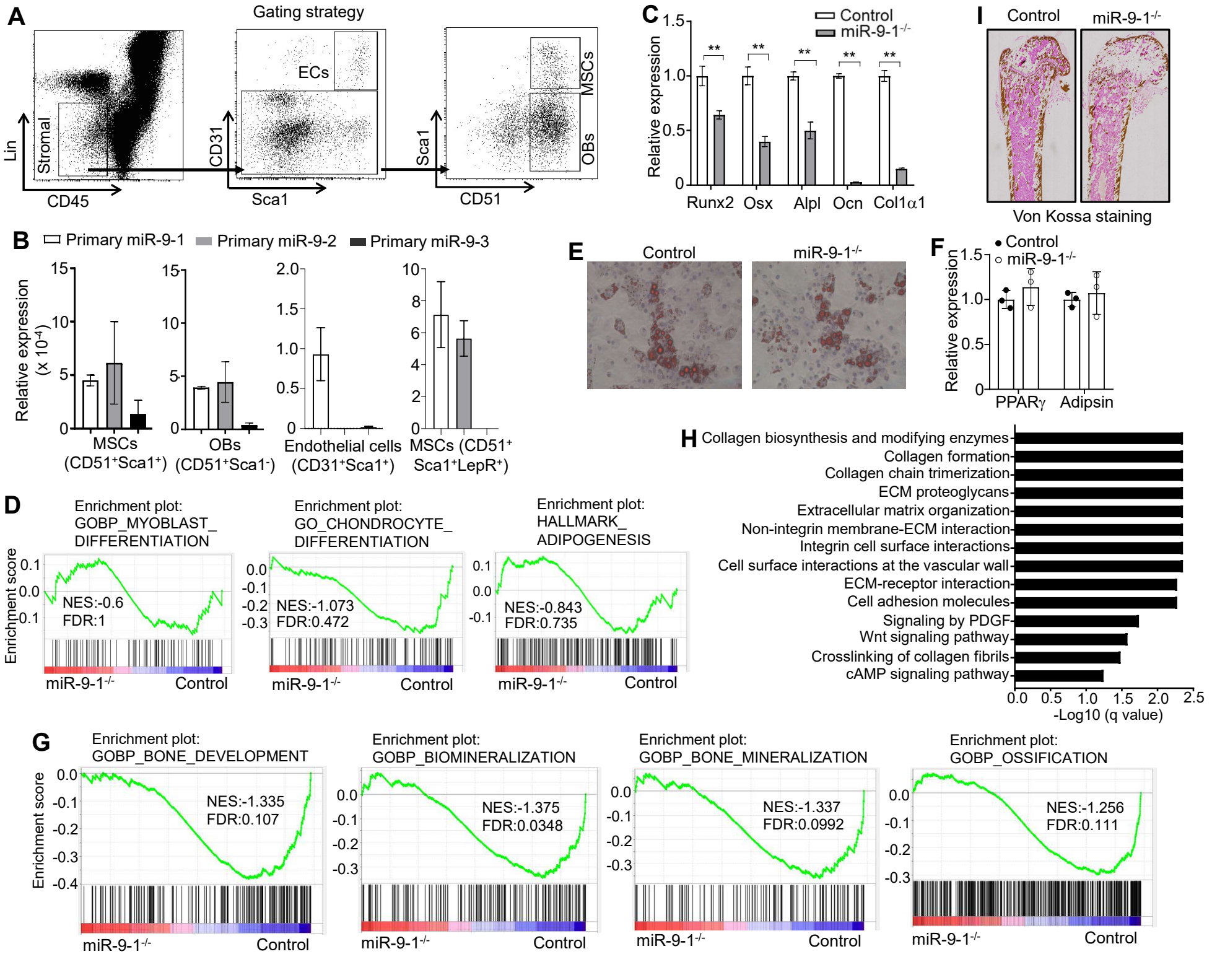
A
Gating strategy
Lin
Stromal
CD45
CD31
ECs
Sca1
Sca1
MSCs
OBs
CD51
B
Primary miR-9-1
Primary miR-9-2
Primary miR-9-3
Relative expression (x 10⁻⁴)
MSCs (CD51⁺Sca1⁺)
OBs (CD51⁺Sca1⁻)
Endothelial cells (CD31⁺Sca1⁺)
MSCs (CD51⁺ Sca1⁺LepR⁺)
C
Control
miR-9-1⁻/⁻
Relative expression
Runx2
Osx
Alpl
Ocn
Col1α1
I
Control
miR-9-1⁻/⁻
Von Kossa staining
E
Control
miR-9-1⁻/⁻
F
Control
miR-9-1⁻/⁻
Relative expression
PPARγ
Adipsin
H
Collagen biosynthesis and modifying enzymes
Collagen formation
Collagen chain trimerization
ECM proteoglycans
Extracellular matrix organization
Non-integrin membrane-ECM interaction
Integrin cell surface interactions
Cell surface interactions at the vascular wall
ECM-receptor interaction
Cell adhesion molecules
Signaling by PDGF
Wnt signaling pathway
Crosslinking of collagen fibrils
cAMP signaling pathway
-Log10 (q value)
D
Enrichment plot: GOBP_MYOBLAST_ DIFFERENTIATION
NES:-0.6
FDR:1
Enrichment plot: GO_CHONDROCYTE_ DIFFERENTIATION
NES:-1.073
FDR:0.472
Enrichment plot: HALLMARK_ ADIPOGENESIS
NES:-0.843
FDR:0.735
Enrichment score
miR-9-1⁻/⁻
Control
G
Enrichment plot: GOBP_BONE_DEVELOPMENT
NES:-1.335
FDR:0.107
Enrichment plot: GOBP_BIOMINERALIZATION
NES:-1.375
FDR:0.0348
Enrichment plot: GOBP_BONE_MINERALIZATION
NES:-1.337
FDR:0.0992
Enrichment plot: GOBP_OSSIFICATION
NES:-1.256
FDR:0.111
Enrichment score
miR-9-1⁻/⁻
Control

Supplementary Figure S8. Analysis of gene expression profiles and normal adipogenic differentiation of miR-9-1-deficient MSCs from growth-retarded mutant mice.

(A) FACS sorting of MSCs, OBs, and endothelial cells from BM stromal cells and gating strategy. (B) Expression of miR-9-1, miR-9-2, and miR-9-3 in the BM niche cells. The relative mRNA levels of miR-9-1, miR-9-2 and miR-9-3 in $CD51^+Sca\text{-}1^+$ MSCs, $CD51^+Sca\text{-}1^+LepR^+$ MSCs, and $CD51^+Sca\text{-}1^-$ OBs within the $Lin^-CD45^-CD31^-$ gate, and $CD31^+Sca\text{-}1^+$ endothelial cells within the Lin^-CD45^- gate. (C) The relative mRNA levels of Runx2, Osx, Alp, Ocn, and Col1a1 in miR-9-1-deficient OBs. The mRNA levels of Runx2, Osx, Alp, Ocn, and Col1a1 in sorted miR-9-$1^{-/-}$ OBs ($CD51^+Sca\text{-}1^-$) were quantified by qRT-PCR as a fraction of the corresponding wild-type control cells, which was set as 1. (D) GSEA of the myoblast, chondrocyte and adipocyte signatures in miR-9-$1^{-/-}$ and wild-type control MSCs ($CD51^+Sca\text{-}1^+$). (E, F) Normal adipogenic differentiation of MSCs from growth-retarded miR-9-1-deficient mice. MiR-9-$1^{-/-}$ and control MSCs were cultured in adipogenic media for 7 days. Oil red staining were performed (E), and the mRNA levels of PPARγ and Adipsin in miR-9-$1^{-/-}$ MSCs were quantified by qRT-PCR as a fraction of the corresponding control cells, which was set as 1 (F). (G) GSEA of the bone development, mineralization, and ossification signatures in miR-9-$1^{-/-}$ and wild-type control MSCs. (H) Enrichment analysis of downregulated genes in miR-9-$1^{-/-}$ relative to control MSCs using the REACTOME database. Bar plots show negative log10 of false discovery rate (FDR) q-values for enrichment. (I) Sections of the femurs from 6- to 12-week miR-9-$1^{-/-}$ and control mice were analyzed for bone mineralization by Von Kossa staining. Data shown are obtained from or representative of 4 (A, C, D, G and H) or 3 (I) miR-9-$1^{-/-}$ and wild-type mice or 3 (B) or 2 (E, F) independent experiments.

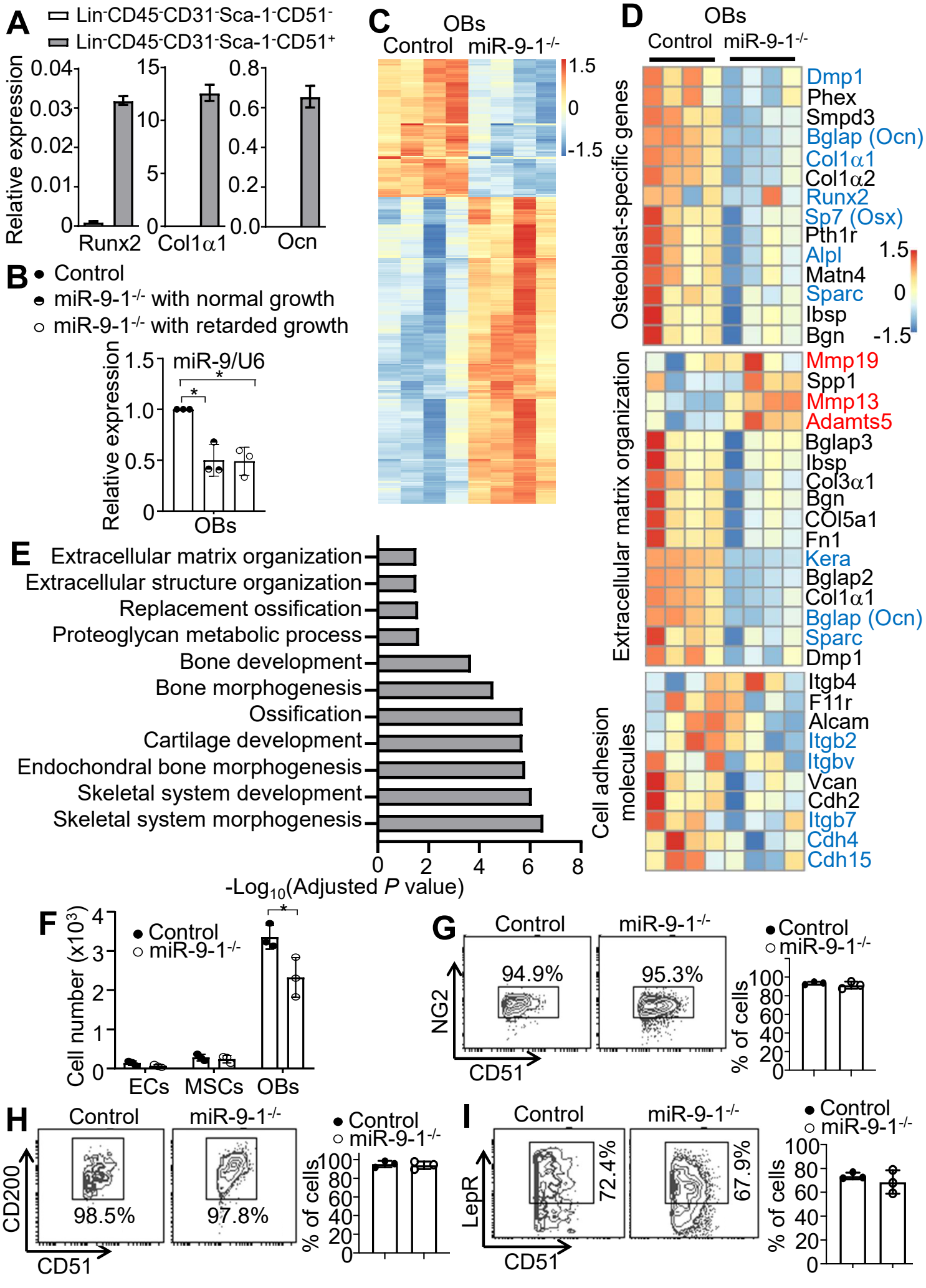
A
Lin-CD45-CD31-Sca-1-CD51-
Lin-CD45-CD31-Sca-1-CD51+
Relative expression
Runx2
Col1α1
Ocn
B
Control
miR-9-1-/- with normal growth
miR-9-1-/- with retarded growth
miR-9/U6
Relative expression
OBs
C
OBs
Control
miR-9-1-/-
D
OBs
Control
miR-9-1-/-
Osteoblast-specific genes
Dmp1
Phex
Smpd3
Bglap (Ocn)
Col1α1
Col1α2
Runx2
Sp7 (Osx)
Pth1r
Alpl
Matn4
Sparc
Ibsp
Bgn
Extracellular matrix organization
Mmp19
Spp1
Mmp13
Adamts5
Bglap3
Ibsp
Col3α1
Bgn
COl5a1
Fn1
Kera
Bglap2
Col1α1
Bglap (Ocn)
Sparc
Dmp1
Cell adhesion molecules
Itgb4
F11r
Alcam
Itgb2
Itgbv
Vcan
Cdh2
Itgb7
Cdh4
Cdh15
E
Extracellular matrix organization
Extracellular structure organization
Replacement ossification
Proteoglycan metabolic process
Bone development
Bone morphogenesis
Ossification
Cartilage development
Endochondral bone morphogenesis
Skeletal system development
Skeletal system morphogenesis
-Log10(Adjusted P value)
F
Control
miR-9-1-/-
Cell number (x10^3)
ECs
MSCs
OBs
G
Control
miR-9-1-/-
94.9%
95.3%
NG2
CD51
% of cells
H
Control
miR-9-1-/-
98.5%
97.8%
CD200
CD51
% of cells
I
Control
miR-9-1-/-
72.4%
67.9%
LepR
CD51
% of cells

Supplementary Figure S9. MiR-9-1 regulates expression of the genes associated with osteoblast differentiation and function in OBs and the populations of NG2$^+$, CD200$^+$, and LepR$^+$ cells within CD51$^+$Sca1$^-$ BM stromal cells in miR-9-1-deficient mice.

(A) The relative mRNA levels of Runx2, Col1a1, and Ocn in sorted OBs were quantified by qRT–PCR using β-Actin as an internal control. Lin$^-$CD45$^-$CD31$^-$Sca-1$^-$CD51$^-$ cells were used as a negative control. (B) The relative levels of total mature miR-9 in OBs from miR-9-1-deficient mice with normal or retarded growth. The levels of total mature miR-9 in sorted OBs from the indicated mice were quantified by qRT-PCR as a fraction of the corresponding wild-type control OBs, which was set as 1. (C) Heatmap of differentially expressed genes between OBs from growth-retarded miR-9-1$^{-/-}$ mice and control mice. Genes with an adjusted p-value < 0.05 found by DESeq2 were assigned as differentially expressed. (D) Heatmap of differentially expressed osteoblast-specific, extracellular organization and cell adhesion molecule genes between OBs from growth-retarded miR-9-1$^{-/-}$ mice and control mice. (E) GO enrichment analysis of downregulated genes in OBs from growth-retarded miR-9-1$^{-/-}$ mice relative to control OBs. Bar plots show negative log10 of p-values for GO enrichment analysis of the biological pathways in control relative to miR-9-1$^{-/-}$ OBs. (F-I) The populations of MSCs, ECs, OBs, and NG2$^+$, CD200$^+$ and LepR$^+$ cells within CD51$^+$Sca1$^-$ BM stromal cells. BM stromal cells from growth-retarded miR-9-1$^{-/-}$ mice and control mice were stained with the anti-lineage cocktail (Mac-1, Gr-1, B220, CD4, CD8, and Ter-119), CD45.2, CD31, CD51, Sca-1, NG2, CD200, and LepR antibodies. The numbers of MSCs, ECs, and OBs were determined (F). The percentages of the indicated cells in the Lin$^-$CD45.2$^-$CD31$^-$CD51$^+$Sca1$^-$ gate were shown (G-I). Data shown is obtained from 4 (A, C-E) or 3 (B, F-I) growth-retarded miR-9-1$^{-/-}$ and wild-type mice. Mean ± SD is shown. *, $p < 0.05$; **, $p < 0.01$.

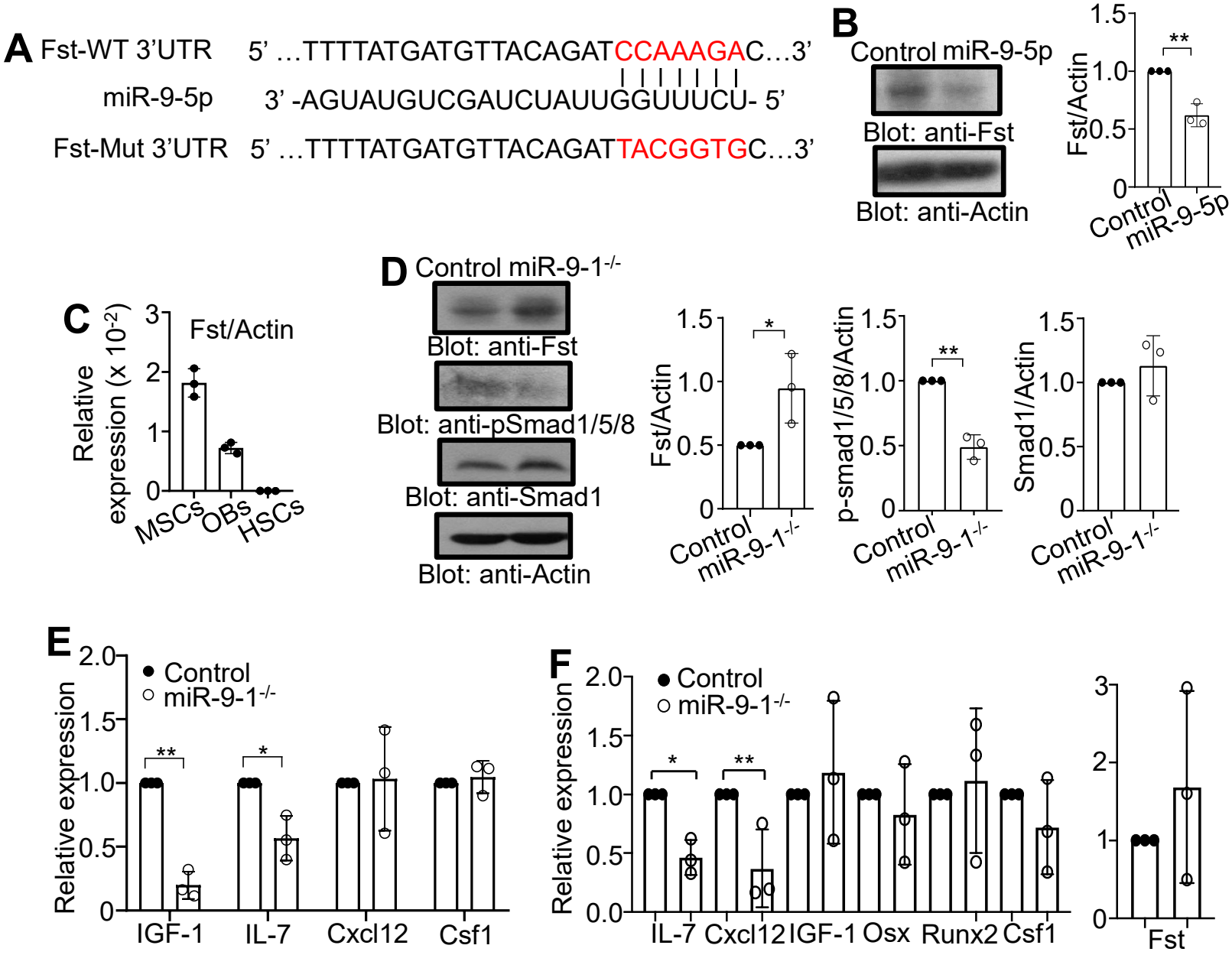
A
Fst-WT 3'UTR 5' …TTTTATGATGTTACAGATCCAAAGAC…3'
miR-9-5p 3' -AGUAUGUCGAUCUAUUGGUUUCU- 5'
Fst-Mut 3'UTR 5' …TTTTATGATGTTACAGATTACGGTGC…3'
B
Control miR-9-5p
Blot: anti-Fst
Blot: anti-Actin
Fst/Actin
Control
miR-9-5p
C
Relative expression (x 10-2)
Fst/Actin
MSCs
OBs
HSCs
D
Control miR-9-1-/-
Blot: anti-Fst
Blot: anti-pSmad1/5/8
Blot: anti-Smad1
Blot: anti-Actin
Fst/Actin
p-smad1/5/8/Actin
Smad1/Actin
Control
miR-9-1-/-
E
Control
miR-9-1-/-
Relative expression
IGF-1
IL-7
Cxcl12
Csf1
F
Control
miR-9-1-/-
Relative expression
IL-7
Cxcl12
IGF-1
Osx
Runx2
Csf1
Fst

Supplementary Figure S10. MiR-9-5p regulates BMP signaling in MSCs by directly targeting Fst.
(A) The predicted Fst 3'-UTR binding site of miR-9-5p and the mutant Fst 3'-UTR binding site of miR-9-5p. (B) Reduced level of endogenous Fst protein in primary MSCs by miR-9-5p overexpression. The expression levels of Fst in MSCs transfected with empty vector (control) or miR-9-5p expression vector (miR-9-5p) was determined by Western-blot (left panel). Band intensity was measured using ImageJ software, and the results are presented as a ratio of the band intensity of Fst to Actin (right panel). (C) The levels of Fst expression in MSCs, OBs and HSCs of wild-type mice. The relative expression levels of Fst were determined in sorted wild-type $CD51^+Sca1^+$ MSCs, $CD51^+Sca1^-$ OBs and HSCs by qRT-PCR analysis. The relative mRNA levels of Fst were normalized to Actin. (D) The protein levels of Fst and phospho-Smad1/5/8 (p-smad1/5/8) in miR-9-1-deficient MSCs. Cell lysates from cultured miR-9-$1^{-/-}$ and control $CD51^+Sca1^+$ MSCs were subjected to Western blot analysis with the indicated antibodies (left panel). The levels of Smad1 and Actin proteins were used as loading controls. Band intensity was measured using ImageJ software, and the results are presented as a ratio of the band intensity of Fst, pSmad1/5/8 or Smad to Actin (right panel). (E) The levels of IGF-1, IL-7, Cxcl12 and Csf1 mRNA in miR-9-$1^{-/-}$ relative to control MSCs. The mRNA levels of IGF-1, IL-7, Cxcl12 and Csf1 in miR-9-$1^{-/-}$ $CD51^+Sca1^+$ MSCs were quantified by qRT-PCR as a fraction of the corresponding control wild-type cells, which was set as 1. The relative mRNA levels of the indicated genes in miR-9-$1^{-/-}$ and control MSCs were normalized to Actin. (F) The levels of IGF-1, IL-7, Cxcl12, Csf1, Osx, Runx2 and Fst mRNA in miR-9-$1^{-/-}$ relative to control $LepR^+$ cells. BM $Lin^-CD45^-CD31^-$ $CD51^+LepR^+$ cells were sorted from miR-9-$1^{-/-}$ mice with retarded growth and control mice. The mRNA levels of the indicated genes in miR-9-$1^{-/-}$ $LepR^+$ cells were quantified by qRT-PCR as a fraction of the corresponding control wild-type cells, which was set as 1. The relative mRNA levels of the indicated genes in miR-9-$1^{-/-}$ and control $LepR^+$ cells were normalized to Actin. Data shown are representative of or obtained from 3 (B, D to F) miR-9-$1^{-/-}$ and control mice, and 3 (C) wild-type mice. Each dot represents an individual mouse. Mean $\pm$ SD is shown. *, $p < 0.05$; **, $p < 0.01$.

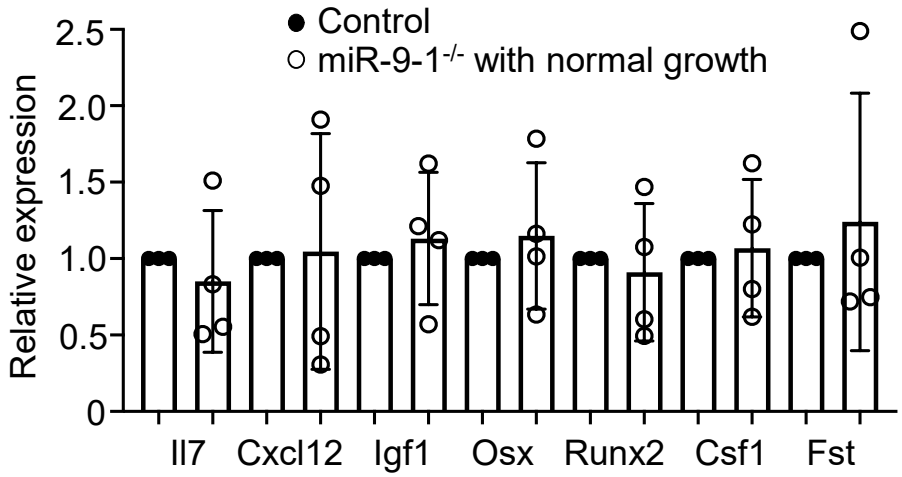

Supplementary Figure S11. The levels of Igf1, IL-7, Cxcl12, Csf1, Osx, Runx2 and Fst mRNA in LepR$^+$ cells from miR-9-1-deficient mice with normal growth relative to control mice.

BM Lin$^-$CD45$^-$CD31$^-$CD51$^+$LepR$^+$ cells were sorted from miR-9-1$^{-/-}$ mice with normal growth and control mice. The mRNA levels of Igf1, IL-7, Cxcl12, Csf1, Osx, Runx2 and Fst in miR-9-1$^{-/-}$ MSCs were quantified by qRT-PCR as a fraction of the corresponding control wild-type cells, which was set as 1. The relative mRNA levels of the indicated genes in miR-9-1$^{-/-}$ and control MSCs were normalized to Actin. Each dot represents an individual mouse, and the mean ± SD is shown.

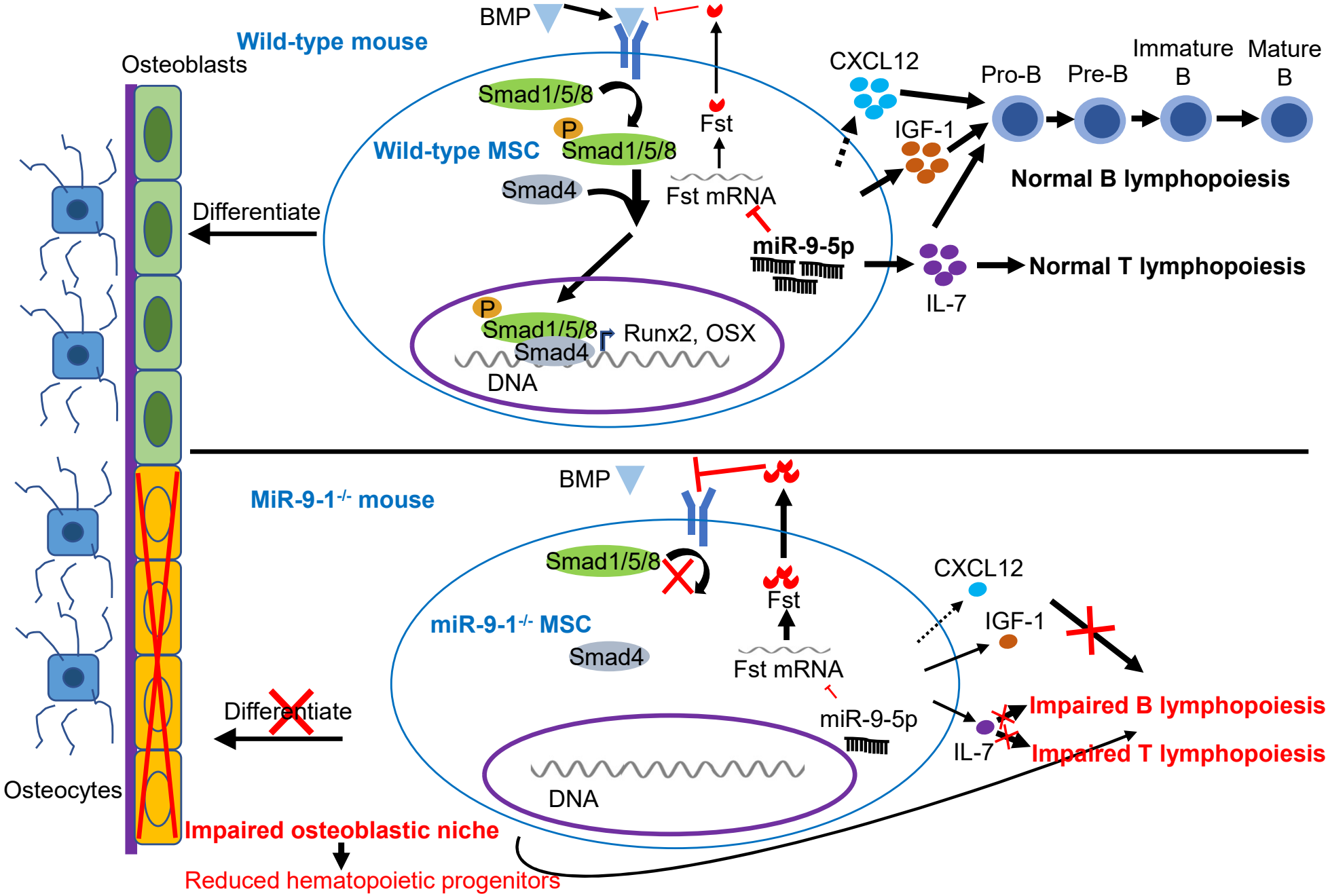

Supplementary Figure S12. Model of miR-9-1 regulation of lymphopoiesis.

MiR-9-1 controls osteoblastic differentiation, at least in part, by downregulating Fst, an antagonist of BMP. When miR-9-1 is deficient, Fst level increases, resulting in reduced BMP signaling, impaired osteoblastic differentiation, and decreased production of IL-7, IGF-1 and possibly CXCL12. Ultimately, this disruption of the osteoblastic niche leads to a reduction in hematopoietic progenitors and impaired lymphopoiesis.